

## Sensor Scheduling Schemes and Network Coverage in Dense Wireless Sensor Networks

SUNANDITA DEBNATH<sup>1,2</sup> AND ASHRAF HOSSAIN<sup>1</sup>

<sup>1</sup>*Department of Electronics and Communication Engineering  
National Institute of Technology Silchar  
Assam, 788010 India*

<sup>2</sup>*Madanapalle Institute of Technology and Science  
Andhra Pradesh, 517325 India*

*E-mail: {sunandita23.1990; ashrafiit}@gmail.com*

Energy optimization is a critical issue in randomly deployed dense wireless sensor networks (WSNs). In dense WSNs, the transmitted signal from a source sensor suffers by the interfering signals from surrounding sensors and unwanted events. In such network scenarios nodes are more likely to become non-functional because of noisy environment and residual battery energy depletion *etc.* This further arises the need for redundant sensor deployment and an energy efficient solution is to schedule sensors to go into sleep state periodically. In this present paper, we address a probabilistic coordinated sensor scheduling scheme to overcome the redundancy in sensor deployment and conserve energy thus extending the overall network lifetime. This scheme uses the concept of inhibition distance of hard-core point process (HCPP) for coordination among sensors with little communication overhead. We analyze the influence of various channel parameters and interferers on sensor activation probability. Further, we perform Monte Carlo simulation and show that the coverage fraction achieved by the coordinated scheduling outperforms random scheduling at same active sensor density. We also study the impact of node failure and  $K$ -coverage degree on the achievable coverage fraction in interference limited WSNs.

**Keywords:** coordinated sensor scheduling, hard-core point process, coverage fraction, interference sensing channel model, node failure

### 1. INTRODUCTION

In recent decades, wireless sensor networks (WSNs) have emerged as a critical area of research for variety of applications starting from military surveillance to health care monitoring, transportation traffic monitoring, smart home and offices *etc.* A sensor network has to be highly self-organizing as most of the time the sensor nodes remain unattended for a longer period of time. In such network scenarios sensors often have limited battery energy which are not replaceable and rechargeable, affecting coverage and lifetime of the overall network. Therefore, energy conservation is a critical issue for design consideration in many WSN applications.

Network coverage and connectivity are of paramount importance for measuring the quality of surveillance (QoS) offered by the sensor network. The coverage performance of a sensor network depends on several factors including the node sensing model used to design the network model [1]. To achieve a desired coverage fraction in energy-constrained sensor networks, huge amount of low power sensors are deployed in the targeted

region of interest (RoI). The energy consumed by the individual nodes increases the overall network cost. To make WSN, a cost effective technology energy saving is the most important requirement [2]. In densely deployed sensor networks, all the sensors are not needed to be active at all times as several sensors may redundantly cover the same location. To overcome this sensor redundancy and conserve energy, an energy-efficient approach is to implement sensor scheduling schemes by turning on and off only a subset of sensors.

Several authors in [3-8] have discussed many sleep scheduling schemes for densely deployed WSNs. They are broadly classified into random scheduling and coordinated scheduling schemes. However, the selection of the set of sensors to make active or asleep affects the overall network performance [5]. In random scheduling (RS) scheme, nodes are activated randomly with certain probability without any coordination with their neighbouring sensors. However, this energy conserving RS scheme cannot provide guarantee of adequate coverage, as a result critical events may miss unless all the sensors are on. On the contrary, in coordinated scheduling scheme, sensors need to communicate with their neighbouring sensors to get their exact locations and their state. Jaleel and Egerstedt [9] have proposed a coordinated scheduling scheme using tools from stochastic geometry, while they have considered fixed range sensors for coverage analysis of the network. They have neglected the inherent effect of interference on the sensing coverage of sensors in dense WSNs.

It is found that most of the studies on sensor scheduling schemes have considered only the fixed radius Boolean sensing model to design their network model, neglecting the inherent effect of channel randomness on sensing signal strength and have ensured only 1-coverage to the monitored RoI. Probabilistic sensing models viz. Elfes [10], shadow fading [11], and Lognormal shadowing fading and Rayleigh fading [12] sensing models have also been widely adopted and explored for coverage analysis of WSNs. These models consider realistic sensing range of sensors subject to inherent randomness of the propagation environment and path loss effects. In dense WSNs, sensors also suffer from the interference or interferences caused by simultaneous transmissions of neighbouring sensors or transmitters within the same frequency band. In such network scenarios, there is high probability that a node to become non-functional. On the other hand, some WSN applications demand higher accuracy of coverage such as border security surveillance, target tracking, and intruder detection. To achieve  $K$ -coverage ( $K > 1$ ), each and every point in the region of interest should be under the observable area of at least  $K$  active sensors [13]. A lot of research has already been done focusing  $K$ -coverage of the targeted field and at the same time maintaining  $K$ -connectivity [14-16] considering only the idealistic Boolean sensing model.

In this paper, we have introduced probabilistic coordinated scheduling scheme for sensor activation to meet desired coverage in dense WSNs. The sensor activation is scheduled using the concept of inhibition distance of hard-core point process (HCPP) from stochastic geometry. A network with high sensor density is usually subjected to interference from the neighbouring transmitting sensors. The interference sensing channel model implicitly reflects interference effects on the sensing signal strength of a sensor in dense WSNs. We have investigated how the sensing channel parameters and number of interferers influence the sensor activation probability. Further, we have shown the coverage fraction achieved has been improved by coordinated scheduling of the sen-

sors in comparison to random scheduling while activating same number of sensor nodes. We have also shown the joint impact of coverage degree and node failure probability on coverage fraction in presence of interferers.

The rest of the paper is organized as follows. A brief discussion about related work on node scheduling schemes is presented in Section 2. Section 3 presents the system model and the average sensing radius of sensor in presence of channel randomness and interference. A brief description about the hard-core point process and the probabilistic coordinated scheduling scheme is presented in Section 4. This section presents the various channel parameters influencing the sensor activation probability and the impact of coordinated scheduling scheme on network coverage fraction. The combined effect of node failure probability and coverage degree on coverage fraction in interference limited dense WSN is presented in Section 5. Section 6 presents results and discussions. Finally, Section 7 presents the concluding remarks.

## 2. RELATED WORK

Authors in [17] have proposed an S-MAC protocol for self-organizing WSNs. S-MAC reduces energy consumption by randomly selecting idle nodes to periodically go into sleep mode. By avoiding idle listening this protocol obtains significant energy saving and increases network lifetime. In [18], authors have investigated both random scheduling (RS) and coordinated scheduling algorithms for low duty cycled sensors in the context of network coverage. Duty cycle is the fraction of time a sensor remains in active state. They have concluded that their coordinated scheduling can obtain greater reduction in duty cycle with the same amount of redundancy for fixed network coverage in comparison to RS. Authors in [8] have proposed a Linear distance-based scheduling (LDS) scheme for clustered WSNs and have compared it with the Random scheduling (RS) scheme. In LDS scheme, the sleeping probability of nodes depends on the distance from cluster head (CH), the farther away nodes from CH will go to sleep mode with higher probability and thus balancing energy consumption. This leads to unequal energy consumption by the sensors. To overcome this, authors have further proposed balanced energy scheduling (BS) scheme a special case of DS scheme in [5]. They have derived a sleeping probability function, which no longer depends on the distance from the cluster head. In [19], authors have developed a Traffic-aware density-based sleep scheduling (TDSS) strategy for sensor scheduling considering Gaussian distribution of nodes in a 2-D RoI and compared it with RS, LDS, and BS schemes respectively. This scheme determines the sleeping probability of the sensor nodes considering the node density of an annulus and the relay traffic-load.

Authors in [4] have studied the  $K$ -coverage problem in WSNs and have derived a bound on sensor spatial density to provide  $K$ -coverage to a RoI. Further, they have concluded that to maintain connectivity among the active nodes the communication range must be at least equal to the sensors sensing range. They have proposed four sensor scheduling algorithms to achieve  $K$ -coverage while guaranteeing connectivity. In [20], authors have proposed two methods 3-*Sym* and *O-Sym* of connected  $K$ -coverage assurance for sensor scheduling adapting virtual hexagonal tessellation to divide sensors into groups. These algorithms ensure that each and every sensor node will be selected with

equal probability to become active thus achieving load balancing. In [21], authors have addressed the problem of  $K$ -coverage of a 3-D RoI with heterogeneous sensor nodes considering Boolean sensing model. They have derived the expression of the probability a sensor being redundant for  $K$ -coverage. Further they have proposed a distributed scheduling protocol to reduce the number of active sensors based on the information gathered about the neighbouring nodes only. In [22], authors have proposed a dynamically distributed energy-efficient duty cycle control scheme named Adaptation duty cycle control (ADCC) for energy constrained WSNs based on feedback signals. In this scheme, the duty cycle of sensors is determined based on their real-time residual energy.

The above mentioned algorithms on sensor scheduling have considered only the deterministic sensing model for coverage analysis. These schemes also need the exchange of control overheads for coordination among the sensor nodes, which leads to additional energy consumption. It is found that most of the state-of-the-art works are relied on the deterministic Boolean sensing model. Except in [23-25] authors have evaluated the performance of WSNs employing node scheduling schemes considering probabilistic sensing models. In [23, 24], authors have proposed algorithms to find the set of minimum number of active sensors based on their residual energy to provide full coverage to the monitored point of interests. They have considered the distance-based probabilistic disc sensing model (Elfes sensing model) in their study. Authors in [25] have addressed a novel sensor scheduling scheme to provide  $K$ -coverage to the target event considering Rayleigh fading channel model.

In our work, sensors are scheduled by coordination among them using the concept of inhibition distance from hard-core point process instead of exchanging actual location information. The communication overheads needed for coordination is little that it is comparable to the RS scheme. Further, to design our network model while scheduling we have considered the interference effect on the sensing signal strength of sensors. We have also shown the impact of sensing channel parameters, number of interferers, and node failure probability on network coverage fraction.

### 3. SYSTEM MODEL

We have assumed that sensor nodes are distributed in a random fashion with uniform density in a Poisson field of nodes. In such networks, coverage is one of the performance criterion offered by the deployed sensor network. A point is said to be covered if it falls under the sensing range of at least one of the active sensor nodes in the deployed region. We have considered that the sensor nodes are all static and homogeneous in characteristics with same threshold power. In dense WSNs, a receiver sensor usually suffers by the interference from neighbouring transmitters or sensors transmitting simultaneously within the same frequency band. The aggregated interference at a receiver depends on the spatial distribution and density of interferers in the Poisson field of interest [26]. Therefore, the sensing signal of a node suffers from path loss, shadowing loss, multipath effects and apart from these also suffers from interference (Fig. 1) from surrounding unwanted events in dense WSNs [27].

Thus, the sensing radius of a node in interference limited dense WSNs is nonuniform in all directions unlike the deterministic Boolean sensing model. In densely de-

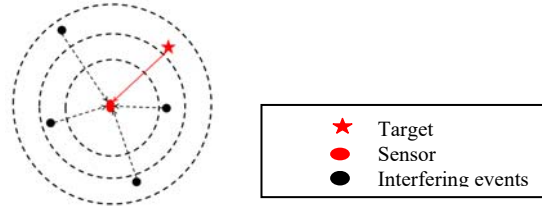


Fig. 1. Interference effects on the receiver sensor from the surrounding events, we assume the receiver is placed on the origin of the coordinate.

ployed networks, the cochannel interference strongly depends on the large scale signal variations caused by shadowing [28]. The received signals by the intended receiver sensor may be correlated, since the signals may be shadowed by the same source of obstacles in the neighbourhood. Dayya and Beaulieu [29] for the first time have addressed the correlation between the interfering signals and between the desired and sum of resulting interfering signals. Kumar & Lobiyal [27] have derived the expression for average sensing radius of sensors in presence of correlated interfering signals and have expressed as

$$r_s = \sqrt{Q \left[ \frac{\ln \lambda' - \ln \left( \frac{a^2}{\sqrt{b}} \right)}{\sqrt{c^2 \sigma^2 + \left( \ln \left( \frac{b}{a^2} \right) \right)^2 - 2\rho c \sigma \ln \left( \frac{b}{a^2} \right)}} \right]} R_{\max}. \tag{1}$$

We have derived a corrected form of  $r_s$  in presence of correlated interfering signals from  $k$  interferers in [30] and have reproduced here for convenience.

$$r_s = \sqrt{Q \left[ \frac{\ln \lambda' + \ln \left( \frac{a^2}{\sqrt{b}} \right)}{\sqrt{c^2 \sigma^2 + \ln \left( \frac{b}{a^2} \right) - 2\rho c \sigma \sqrt{\ln \left( \frac{b}{a^2} \right)}} \right]} R_{\max}. \tag{2}$$

where  $a$  and  $b$  are the first and second moments of sum of correlated lognormal random variables using Wilkinson’s approach [29]. Interfering signals are often modeled as the lognormal random variables.

$$\begin{aligned} a &= k e^{\frac{\sigma^2}{2}} \\ b &= k e^{2\sigma^2} + k^2 e^{\sigma^2(1+\rho)} \end{aligned} \tag{3}$$

$Q(x)$  is defined as  $Q(x) = \frac{1}{\sqrt{2\pi}} \int_x^\infty e^{-y^2/2} dy$ . Here, it is assumed that the desired signal and all the  $k$  interfering signals have zero mean and same variance, correlation coefficient between all interfering signals, and between desired signal and all interfering signals are all same *i.e.*  $\rho$  [27].  $\sigma$  is the standard deviation of shadow fading,  $k$  represents the number of interferers,  $c = 10 \log_e \frac{1}{10}$ ,  $\lambda'$  is the predefined threshold SIR (signal to in-

terference ratio). The definitions of the notations used are presented in Table 1 for ready reference.

**Table 1. Definition of the notation used for the system model.**

Notation	Definition
$\mathcal{L}$	SIR threshold at the receiver sensor
$k$	Number of interferers
$\sigma$	Standard deviation of shadow fading in dB
$\rho$	Correlation coefficient
$R_{\max}$	Maximum practicable sensing radius of a node
$\lambda$	Sensor node density ( $N/A$ )

## 4. SCHEDULING SCHEME

In this section, first we have described the hard-core point process from which the concept of inhibition distance is employed for sensor scheduling then we have presented our proposed probabilistic coordinated scheduling scheme for sensors in section 4.2.

### 4.1 Hard-core Point Process

The nodes locations in a randomly deployed stationary WSN can be modeled as a Poisson point process (PPP)  $\Phi$  of density  $\lambda$ , expected number of nodes per unit area. To model the distribution of randomly and uniformly deployed sensors as spatial Poisson point process has received intense attention in the literature of WSNs. Moreover, if the sensors are distributed with a constant density  $\lambda$  throughout the RoI, then it can be modeled as a Homogenous Poisson point process (HPPP). A number of more complicated point processes can be derived from the parent Poisson point process. A fundamental operation thinning can be performed on the parent PPP to generate new point processes. Thinning is done by randomly deleting a point with some deterministic probability  $(1-p)$ , where  $p$  represents the retention probability, and the deletion of each point is independent of deleting or retaining other points of  $\Phi$ . This well-known independent thinning is called as  $p$ -thinning or  $p(x)$  thinning; apart from this there also exists distance-dependent thinning. Our work is concentrated on dependent thinning more specifically distance-dependent thinning. This distance-dependent thinning is also known as the widely accepted Matern hard-core point process (MPP). Matern first and second order hard-core point processes are the examples of dependent thinning [31]. Here, two points are forbidden to lie closer than a minimum hard-core distance,  $d'$  which is called the inhibition distance. In Matern I hard-core process, every point of  $\Phi$  is deleted in the process if the pair wise distances between the constituent points are less than the specified hard-core distance,  $d'$ . On the other hand, in Matern II hard-core process each point of  $\Phi$  is associated with independent random time mark. The random time mark is uniformly distributed in  $[0, 1]$ . The point with the smallest time mark in the inhibition range is retained and all other points are eliminated.

### 4.2 Probabilistic Coordinated Sensor Scheduling Scheme

To maintain a desired level of coverage especially in applications (*e.g.* forest fire

detection, military surveillance, home security, and environmental hazardous monitoring *etc.*) a huge number of nodes have to be deployed, which also leads to huge energy consumption and a high network cost. An efficient approach to minimize sensor redundancy and overall energy consumption is to implement sensor scheduling schemes. An energy efficient scheduling scheme should minimize sensor redundancy while maintaining the desired coverage fraction. The expression for coverage fraction in randomly deployed sensor networks can be represented as

$$P_{cov} = 1 - e^{-NP_{det}}. \tag{4}$$

Here  $P_{det}$  is the detection probability of a sensor in presence of  $k$  interferers and is  $\pi r_s^2/A$ ,  $A$  denotes area of the RoI.  $P_{cov}$  in Eq. (4) will reduce with the increase in number of interferers ( $k$ ). This is because with the increase in number of interferers the average sensing radius of the sensor reduces.

For random scheduling scheme, the expression for  $P_{cov}$  can be expressed as

$$P_{cov} = 1 - e^{-\lambda \pi r_s^2 P_r}. \tag{5}$$

where  $P_r (\in [0,1])$  is the probability of a sensor node to be in on state, then  $(1 - P_r)$  represents the probability to be in off state. A sensor decides its states randomly depending on the value of  $P_r$ , whether to be turn on or off. Random scheduling scheme is energy efficient in the sense that the sensors need not to communicate with their neighbouring sensors. As a result of this critical events may miss out if the corresponding sensor is off. Thus, in our work we have adopted coordinated scheduling scheme to activate minimum number of sensors with probabilistic sensing range in interference limited dense WSN. For this we have employed the concept of hard-core point process from stochastic geometry. Using the inhibition distance from hard-core point process two simultaneously active sensors are inhibited by communicating a random time mark. Inhibition distance is the minimum allowable distance between two simultaneously active sensors and in our case, it is the average sensing radius of sensors ( $r_s$ ). A random time mark  $m_i$  is assigned to every sensor and the sensor with the lowest mark in the inhibition range  $r_s$  is being activated.  $m_i$  are random numbers uniformly distributed between 0 and 1. Since only random numbers are communicated for coordination among the neighbouring sensors instead of their actual location information, the communication overheads are effectively reduced. The probability of sensors to be in on state defined as the sensor activation probability ( $P_\psi$ ) using probabilistic hard-core coordinated scheduling (HCCS) scheme can be expressed as

$$P_\psi = \int_{m_0=0}^1 q(m_0) dm_0, \tag{6}$$

$$P_\psi = \int_{m_0=0}^1 \left\{ \sum_{N=0}^{\infty} \frac{e^{-\lambda \pi r_s^2} (\lambda \pi r_s^2)^N}{N!} (1 - m_0)^N \right\} dm_0 \tag{7}$$

where  $q(m_0)$  is the probability that a sensor with mark  $m_0$  will remain on in area  $\pi r_s^2$ .  $m_0$  is uniformly distributed in  $[0, 1]$ . For large values of  $N$ , Eq. (7) reduces to

$$P_\psi = \int_{m_0=0}^1 e^{-\lambda\pi r_s^2 m_0} dm_0 \tag{8}$$

After simplification we get

$$P_\psi = \frac{1 - \exp(-\lambda\pi r_s^2)}{\lambda\pi r_s^2} \tag{9}$$

Eq. (9) can be directly followed from the properties of hard-core point process from stochastic geometry [32]. Substituting the expression of  $r_s$  from Eq. (2) in Eq. (9), the sensor activation probability ( $P_\psi$ ) for dense WSNs in presence of  $k$  interferers is

$$P_\psi = \frac{1 - \exp\left(-\lambda\pi R_{\max}^2 Q \left( \frac{\ln \lambda' + \ln\left(\frac{a^2}{\sqrt{b}}\right)}{\sqrt{c^2\sigma^2 + \ln\left(\frac{b}{a^2}\right) - 2\rho c\sigma\sqrt{\ln\left(\frac{b}{a^2}\right)}}}\right)\right)}{\lambda\pi R_{\max}^2 Q \left( \frac{\ln \lambda' + \ln\left(\frac{a^2}{\sqrt{b}}\right)}{\sqrt{c^2\sigma^2 + \ln\left(\frac{b}{a^2}\right) - 2\rho c\sigma\sqrt{\ln\left(\frac{b}{a^2}\right)}}}\right)} \tag{10}$$

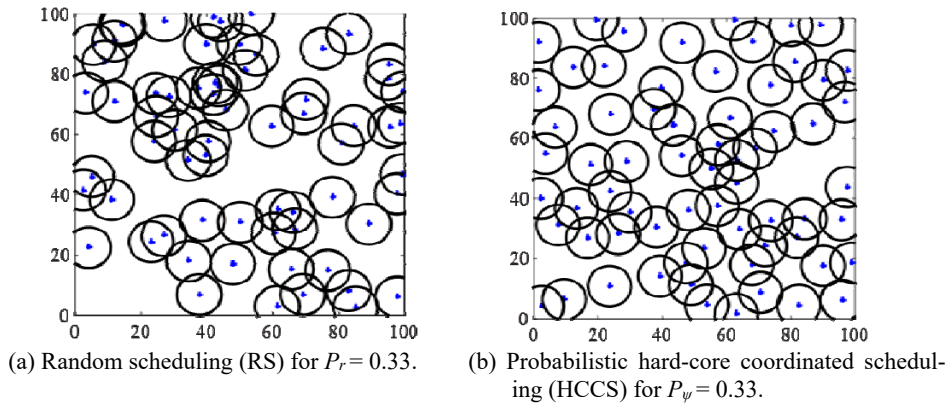


Fig. 2. Comparison between the distribution of active sensor nodes in presence of  $k = 6$  number of interferers.

Figs. 2 (a) and (b) demonstrate the possible distribution of active sensors under random scheduling (RS) and probabilistic hard-core coordinated scheduling (HCCS) schemes simulated in MATLAB under same sensor activation probability  $P_r = P_\psi = 0.33$ . HCCS scheme is simulated with inhibition distance  $d' = r_s$ . The circles represent the footprints of active sensors. It is obvious from the figure that the coverage area has increased for probabilistic HCCS scheme in comparison to RS scheme for equal number of active sensors. Put another way, for a desired coverage the number of nodes required by HCCS

scheme is much smaller than the RS scheme. This in a subtle way also reduces the interference effects by reducing the number of active sensors. For clarity of understanding and implementation the basic form of probabilistic hard-core scheduling scheme is presented in Algorithm 1.

---

**Algorithm 1: Coordinated Scheduling Scheme**

---

**Inputs:**  $\sigma, \lambda', \rho, k, R_{max}, A, K$  and  $P_f$   
**Process** **Step 1:** compute the average sensing radius  $r_s$  in presence of  $k$  interferers according to Eq. (2)  
**Step 2:** deploy  $N$  sensor nodes randomly following Poisson distribution of intensity  $\lambda$   
**Step 3:** select a sensor randomly from  $N$  deployed sensors, say the selected sensor  $x_i$  is located at location  $i$  ( $i \in 1, 2, \dots, N$ )  
**Step 4:** generate and assign independent random variable  $m_i$  to all the neighbouring sensors of node  $x_i$ , where  $m_i$  is uniformly distributed between 0 and 1 i.e.  $m_i \sim unif[0, 1]$

$$N_d(x_i) = \{x_j: \text{for all } x_j \in B(x_i, r_s) \cap \phi\} \text{ and } i \neq j$$

Here  $N_d(x_i)$  denotes set of the neighbouring sensors of the selected sensor  $x_i$  and  $B(x_i, r_s)$  is the sensing region of  $x_i$  with radius  $r_s$

**Step 5:** the sensor with mark  $m_i$  will become active if

$$m_i < m_j \quad \text{for all } j \in N_d(x_i)$$

**Step 6:** repeat this process for all the deployed  $N$  sensor nodes

**Step 7:** run steps 1 to 4 for 1000 iterations and average the results to get the coverage curve for probabilistic HCCS scheme

---

To further validate the performance of our proposed scheme over RS scheme, we have resorted to the concept of deployment entropy first introduced in [33] to investigate the quality of coverage for a given sensor deployment. In [34], authors have evaluated the deployment entropy to measure the quality of sensor deployment in a region of interest by partitioning the RoI into concentric virtual hexagonal structures. Hexagonal structures are the most universally accepted structures for wireless communication networks. The expression for deployment entropy is same as the information entropy as reported in [33] and can be represented here as

$$H = -\sum_{l=1}^{n_s} p_l \log_e p_l \tag{11}$$

where  $p_l = \frac{r_l}{\sum_{q=1}^{n_s} r_q}$  (12)

In Eq. (12),  $r_l$  represents the ratio of number of sensors over the area of  $l$ th concentric hexagonal cell and  $\sum_{q=1}^{n_s} r_q$  is the sum of all such ratios.  $n_s$  is the number of concentric hexagonal cells.  $H$  attains maximum value when all events are equiprobable and it is possible when the sensors are approximately uniformly distributed. Higher value of  $H$  implies

more sensing coverage. The significance of evaluating deployment entropy to measure the sensor distribution after sensor scheduling is presented in Section 6.3.

#### ➤ Node Saving Ratio

To obtain a desired coverage fraction  $P_{cov} = P_{des}$ , the number of nodes required to be active for random scheduling as well as for probabilistic HCCS schemes are  $NP_r$  and  $NP_\psi$  respectively. For a fixed  $P_{des}$ , the required  $P_r$  and  $P_\psi$  can be computed from Eqs. (5) and (10). To compare the performance of probabilistic HCCS over RS, we have calculated the node saving ratio ( $\psi$ ) and can be expressed as

$$\psi = \frac{(P_r - P_\psi)}{P_r}. \quad (13)$$

#### ➤ Network Lifetime

To further validate the supremacy of our proposed scheme over the random scheduling (RS) scheme, we have analyzed the lifetime of the deployed network for both the scheduling schemes. For RS scheme the energy consumption is only due to sensing of the circular region of radius  $r_s$ . Therefore, energy consumption model for RS scheme can be expressed as

$$E_s = \alpha r_s^\eta T_s \quad (14)$$

where  $\alpha$  is the constant for power density of sensor,  $\eta$  is the path loss exponent,  $T_s$  is the time interval for which the sensor remains active. The sensor will dissipate energy only in active state. On contrary to RS scheme, the energy consumption for probabilistic HCCS scheme is due to both sensing and transmission of random numbers between the neighbouring nodes within the inhibition range. Therefore, the energy model for HCCS can be represented as

$$E_t = E_s + E_c \quad (15)$$

where  $E_c$  is the energy required for communication between nodes and is given by

$$E_c = m(e_t + e_d r_s^\eta). \quad (16)$$

Here  $m$  is the number of transmitted bits. In our model, we have considered that the random numbers are 8 bits uniformly distributed numbers, so that the proposed scheme can be implementable using an 8-bit processor. The term  $e_t$  and  $e_d$  are radio parameters [35].

The network lifetime can be expressed as the number of data gathering cycles ( $T_d$ ) the network will survive [36]. In other words, after  $T_d$  data gathering cycles the network will become non-functional due to battery energy depletion of the sensor nodes. Therefore, the network lifetime for RS scheme can be expressed as

$$T_d = \frac{E_0}{P_r E_s} \quad (17)$$

where  $E_0$  is the initial energy of the deployed network. We have considered that all the

sensor nodes have same initial energy. Similarly, for HCCS scheme network lifetime ( $T_d$ ) can be expressed as

$$T_d = \frac{E_0}{(P_\psi E_s + E_c)}. \quad (18)$$

In Section 6.2, we have shown that though our proposed probabilistic HCCS scheme needs communication overheads for synchronization among the neighbouring sensors, the lifetime achieved by the network using RS and HCCS schemes is approximately same.

## 5. EFFECT OF NODE FAILURE ON $K$ -COVERAGE TO A TARGETED EVENT

In this section, we have shown the combined effect of node failure and coverage degree on coverage fraction in interference limited sensor networks. To provide  $K$ -coverage to a region of interest (RoI) a usual approach found in literature is to add sensor redundancy in the deployed network. On the other hand, in such densely deployed sensor networks, interference is an inherent source of performance degradation. A substantial amount of nodes may become non-functional due to harsh environment condition, software and hardware problems, limited battery energy *etc.* In a network of energy-constrained sensor nodes, a node will fail to detect an event in two conditions: (a) the event to be detected does not lie within the sensing area of the node; (b) event lies within the sensing area and the node fails to detect. Let  $P_f$  be the probability of node failure, then the probability of no node failure is  $(1 - P_f)$ . In presence of node failure, the probability that an event will not be detected by a sensor node is given by [1]

$$P_{undet} = 1 - P_{det}(1 - P_f) \quad (19)$$

Here  $P_{det}$  is the detection probability of a sensor node. Substituting  $r_s$  from Eq. (2),  $P_{undet}$  in presence of  $k$  interferers is

$$P_{undet} = \left\{ 1 - \frac{\pi R_{\max}^2}{A} Q \left( \frac{\ln \lambda' + \ln \left( \frac{a^2}{\sqrt{b}} \right)}{\sqrt{c^2 \sigma^2 + \ln \left( \frac{b}{a^2} \right) - 2\rho c \sigma \sqrt{\ln \left( \frac{b}{a^2} \right)}}} \right) (1 - P_f) \right\}. \quad (20)$$

Therefore, the coverage fraction in presence of  $k$  interferers and node failure can be expressed as

$$P_{cov} = 1 - \left\{ 1 - \frac{\pi R_{\max}^2}{A} Q \left( \frac{\ln \lambda' + \ln \left( \frac{a^2}{\sqrt{b}} \right)}{\sqrt{c^2 \sigma^2 + \ln \left( \frac{b}{a^2} \right) - 2\rho c \sigma \sqrt{\ln \left( \frac{b}{a^2} \right)}}} \right) (1 - P_f) \right\}^N. \quad (21)$$

Eq. (21) ensures 1-coverage to the region of interest by the deployed network. A network to be fault tolerable, each and every location of the field has to be  $K$ -covered, where  $K$  is configurable according to the desired accuracy of detection demanded by the network applications. The degree of coverage can be considered as a measure of QoS that a sensor network provides [13]. Following [37], the expression for  $K$ -coverage probability in presence of node failure  $P_f$  can be represented as

$$P_{cov} = \sum_{M=K}^N C_N^M \left[ \left\{ P_{det} (1 - P_f) \right\}^M \left\{ 1 - P_{det} (1 - P_f) \right\}^{N-M} \right] \quad (22)$$

where  $N$  is total number of randomly deployed sensor nodes.

In network environments where nodes are prone to failure a large value of  $K$  is desired. To ensure  $K$ -coverage to a targeted event while sensor scheduling we have considered the inhibition distance between the sensors to be the average sensing radius  $r_s$ . This will ensure that no critical event to be missed during sensor scheduling and at the same time providing  $K$ -coverage while activating minimum number of sensor nodes. For coverage degree  $K = 3$ , the coverage fraction  $P_{cov}$  achieved after sensor scheduling can be expressed as

$$P_{cov} = 1 - \left\{ 1 - P_{det} (1 - P_f) \right\}^{N_{active}} - N_{active} P_{det} (1 - P_f) \left\{ 1 - P_{det} (1 - P_f) \right\}^{N_{active}-1} - \frac{N_{active} (N_{active} - 1)}{2} \left\{ P_{det} (1 - P_f) \right\}^2 \left\{ 1 - P_{det} (1 - P_f) \right\}^{N_{active}-2} \quad (23)$$

where  $N_{active}$  is number of active sensor nodes after scheduling.

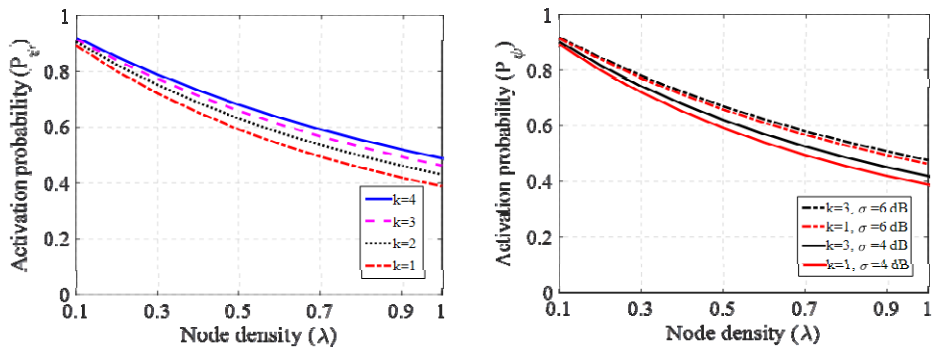
## 6. RESULT AND DISCUSSIONS

### 6.1 Sensor Activation Probability in Presence of Interferers

In this sub-section, firstly we have examined the impact of sensing channel parameters and interferers on sensor activation probability to the sensor node density. The entire sensing region of interest (RoI) is assumed to be a rectilinear field with area  $A = 50 \times 50\text{m}^2$ . Here, we have assumed the maximum number of interferers can be  $k = 6$ . The maximum practicable sensing radius  $R_{max}$  is considered to be 1m and other system parameters used for performance analysis are shown in Table 2. We have done the numerical analysis considering a small RoI but these results are also applicable for large area networks.

**Table 2. System parameters for performance analysis.**

Parameter	Value
Fading parameter, $\sigma$	$2 \text{ dB} \leq \sigma \leq 6 \text{ dB}$
Correlation coefficient, $\rho$	$0.1 \leq \rho \leq 1$
SIR threshold of detection, $\lambda'$	0.1
Sensor node density, $\lambda$	$0 < \lambda \leq 1$



(a) Different number of interferers ( $k$ ) and  $\sigma = 4$  dB. (b) different values of  $\sigma$  (in dB) with varying number of interferers ( $k$ ).

Fig. 3. Variation of activation probability ( $P_\psi$ ) with node density ( $\lambda$ ) for  $\rho = 0.5$ .

Fig. 3 (a) shows the variation of activation probability ( $P_\psi$ ) with node density ( $\lambda$ ) for different number of interferers ( $k$ ). Here, we have considered  $\sigma = 4$  dB and  $\rho = 0.5$ . It is observed from figure that more number of sensors are being activated with the increase in number of interferers ( $k$ ). The sensing radius  $r_s$  considered as the inhibition distance between two active sensors degrades gradually due to the undesired interference from the surrounding environment and as a result to maintain desired coverage more number of sensors are being activated. For example, the number of active sensors increases from  $\sim 40\%$  to  $50\%$  for an increase in number of interferers from  $k = 1$  to 4.

Fig. 3 (b) illustrates the variation of sensor activation probability ( $P_\psi$ ) with node density ( $\lambda$ ) for two different values of  $\sigma$  (in dB) and different number of interferers ( $k$ ). It is observed that when  $\sigma$  increases from 4 dB to 6 dB *i.e.* the propagation environment becomes more severe due to fading, the activation probability ( $P_\psi$ ) increases at a given sensor node density ( $\lambda$ ). For example when  $\sigma = 6$  dB,  $P_\psi$  increases by  $\sim 5\%$  and when  $\sigma = 4$  dB,  $P_\psi$  increases by  $\sim 7\%$  for an increase in number of interferers from  $k = 1$  to 3 respectively. It is clear from the figure that when the propagation environment becomes more adverse *i.e.* at  $\sigma = 6$  dB due to shadowing losses of the propagation channel, the effect of number of interferers ( $k$ ) on sensor activation probability ( $P_\psi$ ) becomes less significant. This is due to the fact that when the transmit environment is adversely affected by shadowing the receiver becomes more rigid to the received sensing signal from the source sensor.

Figs. 4 (a) and (b) show the variation of activation probability ( $P_\psi$ ) with node dens-

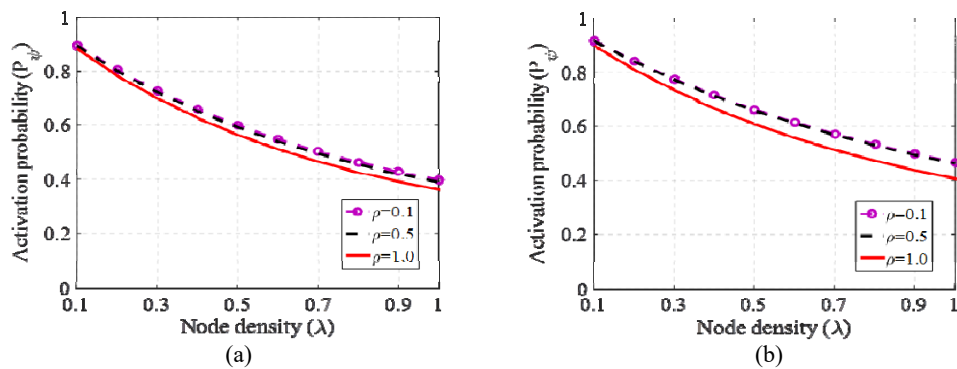


Fig. 4. Variation of activation probability ( $P_\psi$ ) with node density ( $\lambda$ ) for different values of correlation coefficient ( $\rho$ ): (a) interferer  $k = 1$  and  $\sigma = 4$  dB; (b) interferer  $k = 3$  and  $\sigma = 4$  dB.

fity ( $\lambda$ ) for different values of correlation coefficient ( $\rho$ ) and number interferers  $k = 1$  and 3 respectively. It is observed from both the figures that with increase in the value of correlation coefficient  $\rho$ , the sensor activation probability ( $P_\psi$ ) decreases *i.e.* at a given node density ( $\lambda$ ) lesser number of sensors are being activated. For example, when  $\rho$  increases from 0.1 to 1.0 the reduction in  $P_\psi$  is about  $\sim 3.5\%$  at higher node density in presence of  $k = 1$  interferer. In addition, for  $k = 3$  interferers, the percentage reduction in activation probability ( $P_\psi$ ) is about  $\sim 7\%$  for an increase in the value of  $\rho$  from 0.1 to 1.0 at higher node density. It can be concluded from both the figures that with the increase in number of interferers ( $k$ ) the significance of correlation coefficient ( $\rho$ ) becomes more pronounced. These results are obtained for  $\sigma = 4$  dB.

## 6.2 Impact of Node Failure and Coverage Degree on Coverage Fraction without Sensor Scheduling

In this sub-section, we have studied the combined effect of node failure probability ( $P_f$ ) and coverage degree ( $K$ ) on network coverage fraction in presence of interferers. Here, all the system parameters remain same as mentioned in Table 2.

Fig. 5 (a) illustrates the variation of coverage fraction ( $P_{cov}$ ) with number of sensor nodes ( $N$ ) in presence of different number of interferers  $k = 2$  and 6 respectively. Here, the curves are obtained for coverage degree,  $K = 3$ . The solid lines and dashed lines depict the curves for  $k = 2$  and 6 respectively. It is observed that coverage fraction increases with the increase in number of sensor nodes irrespective of the value of node failure probability ( $P_f$ ). For  $P_f = 0$ , *i.e.* in no node failure case and  $N = 300$ , the coverage fraction achieved is  $\sim 94\%$  in presences of  $k = 2$  interferers. It falls to  $\sim 79\%$  and severely degrades to  $\sim 43\%$  for  $P_f = 0.3$  and 0.6 respectively. The decrease in coverage fraction ( $P_{cov}$ ) for first 30% node failure is  $\sim 15\%$  and it is  $\sim 36\%$  for additional 30% node failure. In addition, it is observed that in presence of more number of interferers *i.e.* when  $k = 6$ , the coverage achieved is  $\sim 76\%$  for  $N = 300$  in no node failure case. The coverage fraction further reduces to  $\sim 53\%$  and  $\sim 21\%$  for  $P_f = 0.3$  and 0.6 respectively. It is also clear from figure that slope of the curve has decreased when the number of interferers

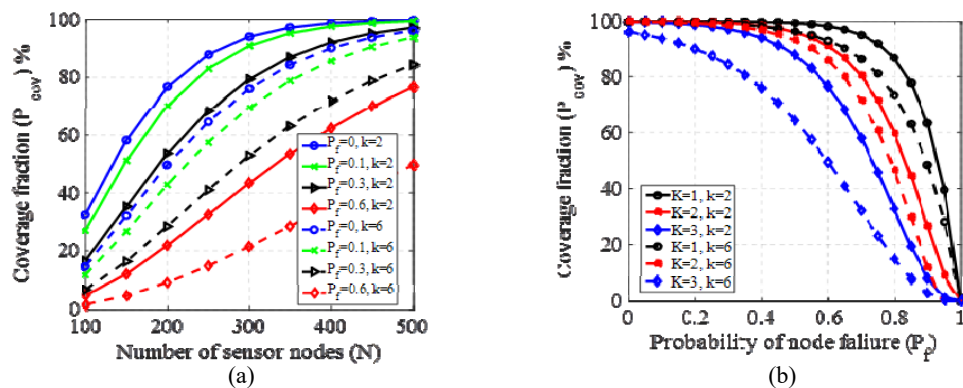


Fig. 5. (a) Coverage fraction ( $P_{cov}$ ) versus number of sensor nodes ( $N$ ) for different values of node failure probability ( $P_f$ ) with coverage degree  $K=3$  and number of interferers  $k = 2$  (solid lines) and  $k = 6$  (dashed lines); (b) Coverage fraction ( $P_{cov}$ ) versus probability of node failure ( $P_f$ ) for different coverage degrees ( $K$ ) and number of interferers  $k = 2$  (solid lines) and  $k = 6$  (dashed lines).

has increased from  $k = 2$  to 6. For  $k = 6$ , the decrease in coverage fraction ( $P_{cov}$ ) for first 30% node failure is  $\sim 23\%$  and it is  $\sim 32\%$  for additional 30% node failure. In addition, even in no node failure case (*i.e.*  $P_f = 0$ ) the decrement in  $P_{cov}$  is about  $\sim 18\%$  when number of interferers increases from  $k = 2$  to 6.

The variation of coverage fraction ( $P_{cov}$ ) with probability of node failure ( $P_f$ ) is shown in Fig. 5 (b) for different number of interferers  $k = 2$  and 6 respectively. It is observed from Fig. 5 (b) that the coverage fraction ( $P_{cov}$ ) is gradually decreasing with the increase in node failure probability ( $P_f$ ). In addition, the coverage fraction further reduces with the increase in coverage degree  $K$ . For coverage degree  $K = 3$ , the sensing coverage reduces from  $\sim 76\%$  to  $\sim 49\%$  for the increase in number of interferers from  $k = 2$  to 6 at  $P_f = 0.6$ . The reduction in coverage fraction ( $P_{cov}$ ) for first 30% node failure is  $\sim 13\%$  and is  $\sim 27\%$  for additional 30% node failure when number of interferers  $k$  increases from 2 to 6. Here also the solid lines and dashed lines represent the curves for  $k = 2$  and 6 respectively.

### 6.3 Impact of Node Failure and Coverage Degree on Coverage Fraction with Sensor Scheduling

To validate the performance of probabilistic coordinated scheduling over random scheduling, we have performed Monte Carlo simulations of the deployed sensor network. The sensing channel parameters considered are  $\sigma = 4$  dB,  $\rho = 0.5$ , and  $\lambda' = 0.1$ . The active sensor node density varies from  $0 < \lambda \leq 0.1$ . To enhance the accuracy of coverage performance ( $P_{cov}$ ) under HCCS and RS schemes at every active node density, the results for  $P_{cov}$  are averaged over 1000 iterations of the simulation. We have done the simulation in MATLAB environment.

The inhibition distance considered for probabilistic coordinated scheduling scheme is the average sensing radius of sensor nodes in presence of  $k$  interferers. We have applied the probabilistic HCCS scheme considering  $d' = r_s$ , and have evaluated the coverage fraction  $P_{cov}$  for  $k = 2$  and 6 interferers respectively. Then, we have used the values of  $P_\psi$  corresponding to  $d' = r_s$  for interferers  $k = 2$  and 6 and have measured  $P_{cov}$  for random scheduling (RS) scheme considering  $P_\psi = P_r$ .

Figs. 6 (a) and (b) show the variation of coverage fraction ( $P_{cov}$ ) with node density ( $\lambda$ ) for coverage degree  $K = 1$  and number of interferers  $k = 2$  for different scheduling schemes in the event of no node failure and 40% node failure.

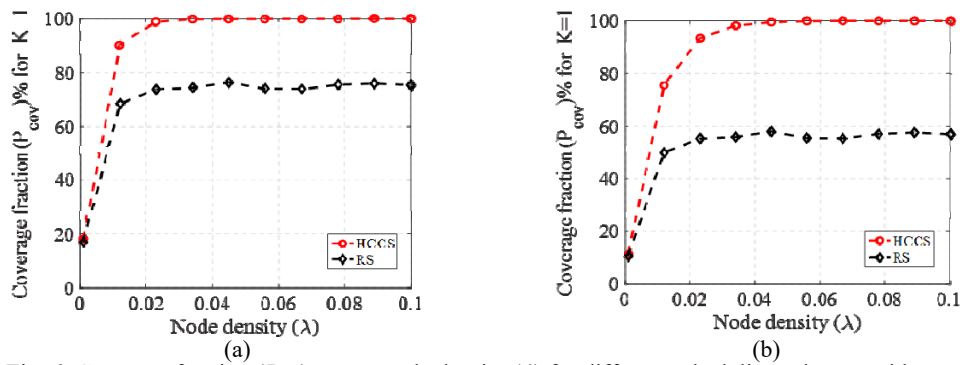


Fig. 6. Coverage fraction ( $P_{cov}$ ) versus node density ( $\lambda$ ) for different scheduling schemes with coverage degree  $K = 1$  and number of interferers  $k = 2$ : (a)  $P_f = 0$  and (b)  $P_f = 0.4$ .

It is observed from Fig. 6 (a) that  $P_{cov}$  achieved for HCCS curve is  $\sim 23\%$  more as compared to RS at active node density  $\lambda = 0.05/\text{m}^2$  in no node failure case (*i.e.*  $P_f = 0$ ). In addition, Fig. 6 (b) shows that for 40% node failure (*i.e.*  $P_f = 0.4$ ) the enhancement in  $P_{cov}$  for probabilistic HCCS scheme is almost  $\sim 41\%$  in comparison to RS scheme at  $\lambda = 0.05/\text{m}^2$ .

The variation of coverage fraction ( $P_{cov}$ ) with node density ( $\lambda$ ) for  $K = 1$  and number of interferers  $k = 6$  is shown in Figs. 7 (a) and (b) for different scheduling schemes.

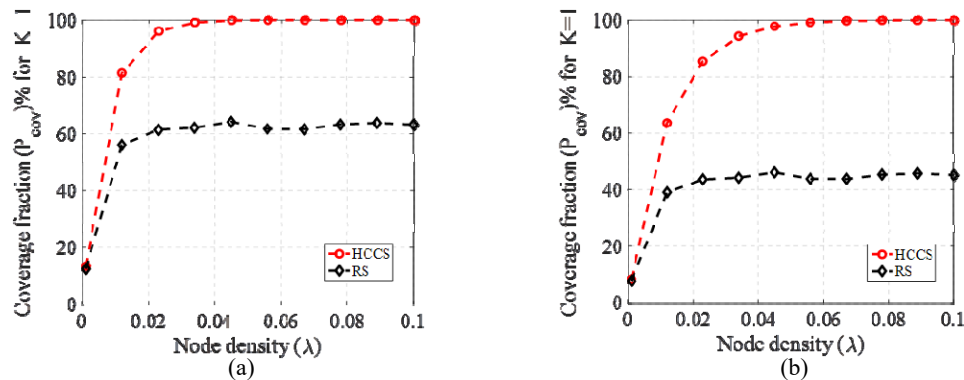


Fig. 7. Coverage fraction ( $P_{cov}$ ) versus node density ( $\lambda$ ) for different scheduling schemes with coverage degree  $K = 1$  and number of interferers  $k = 6$ : (a)  $P_f = 0$  and (b)  $P_f = 0.4$ .

It is observed from both the Figs. 7 (a) and (b) that  $P_{cov}$  decreases in comparison to Figs. 6 (a) and (b) with the increase in number of interferers as expected. In Fig. 7 (a), the achievable coverage ( $P_{cov}$ ) in presence of no node failure (*i.e.*  $P_f = 0$ ) is  $\sim 35\%$  more as compared to RS at active node density  $\lambda = 0.05/\text{m}^2$ . Additionally, it is observed from Fig. 7 (b), that for 40% node failure (*i.e.*  $P_f = 0.4$ ) the enhancement in  $P_{cov}$  for probabilistic HCCS scheme is almost  $\sim 52\%$  in comparison to RS scheme at  $\lambda = 0.05/\text{m}^2$ .

Figs. 8 (a) and (b) show the coverage fraction ( $P_{cov}$ ) for coverage degree  $K = 3$  and  $k = 6$  under different scheduling schemes in the event of no node failure and 40% node failure respectively.

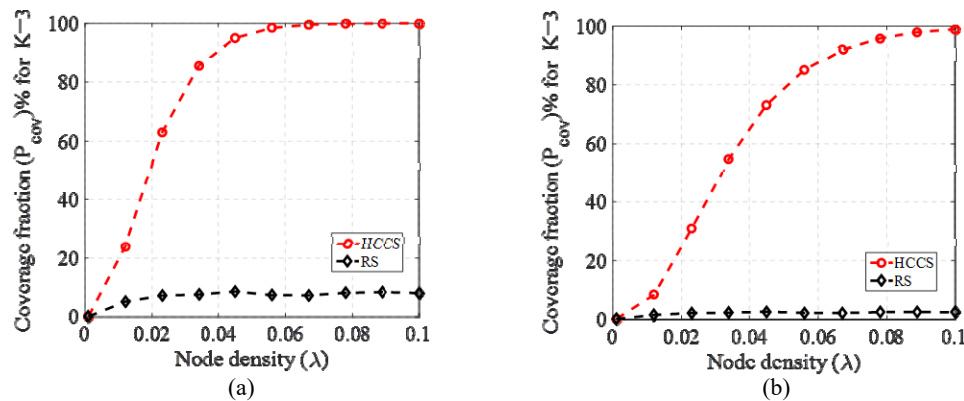


Fig. 8. Coverage fraction ( $P_{cov}$ ) versus node density ( $\lambda$ ) for different scheduling schemes with coverage degree  $K = 3$  and number of interferers  $k = 6$ : (a)  $P_f = 0$  and (b)  $P_f = 0.4$ .

It is observed from Figs. 8 (a) and (b) that for increasing coverage degree (*i.e.*  $K = 3$ ) the coverage fraction ( $P_{cov}$ ) further reduces in comparison to Figs. 6-7 and it degrades severely for RS scheme. Due to nonuniformity in active sensor distribution, the RS scheme fails to provide the desired coverage fraction for increased coverage degree.

Figs. 6-8 show that the probabilistic HCCS scheme outperforms the RS one, due to uniform distribution of the active sensors in the desired RoI as also depicted in Fig. 2. It is clear from the results that in presence of interferers and node failure the random scheduling (RS) scheme provides a poor partial coverage of the RoI. It can be concluded from the results that the sensing channel parameters and node failure probability has a significant impact on the networks achievable coverage. To combat the effect of interference and node failure probability on network coverage some redundant nodes can be deployed and activated by probabilistic HCCS scheme depending on the desired coverage requirements.

To further verify the performance of our proposed scheduling scheme over RS scheme, we have evaluated the deployment entropy to measure the uniformity in active sensor distribution after scheduling. The region of interest of area  $A = 50 \times 50 \text{ m}^2$  is partitioned into five concentric hexagonal cells and 50 sensors are randomly deployed. The number of interferers is considered to be  $k = 6$ . Then both RS and HCCS schemes are implemented on the deployed sensor nodes. Figs. 9 (a) and (b) show the distribution of active sensor nodes in the simulation scenario after sensor scheduling for RS and probabilistic HCCS respectively. The circles with solid lines represent the footprints of active sensors. The values for deployment entropy,  $H$  can be calculated by introducing the ratios of sensors to area of each sub-region in Eq. (11). The computed deployment entropy for RS and probabilistic HCCS schemes are 1.303 and 1.493 respectively. It is also clear from the figure that for HCCS scheme sensors are more uniformly distributed over the entire RoI.

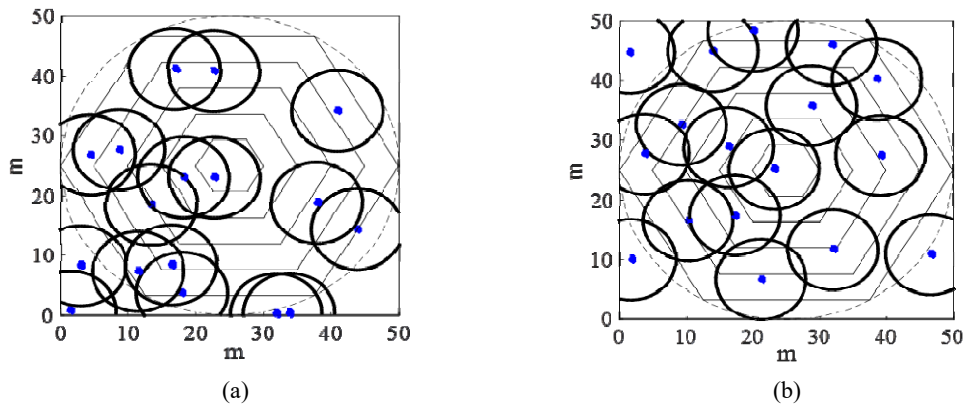


Fig. 9. Distribution of active sensors in concentric hexagonal structure after: (a) Random scheduling (RS) of the sensor nodes (b) Probabilistic hard-core coordinated scheduling (HCCS) of the sensor nodes.

Fig. 10 shows the variation of node saving ratio ( $\psi$ ) for probabilistic HCCS scheme in comparison to RS for different values of desired coverage fraction ( $P_{des}$ ).

It is observed that with the increases in  $P_{des}$ , the node saving ratio ( $\psi$ ) also increases gradually. This is due to the fact that for a fixed sensor density when the desired coverage demanded by an application increases, RS scheme activates more number of sensors in comparison to probabilistic HCCS scheme. Therefore, for higher desired coverage our proposed scheme provides significant performance enhancement.

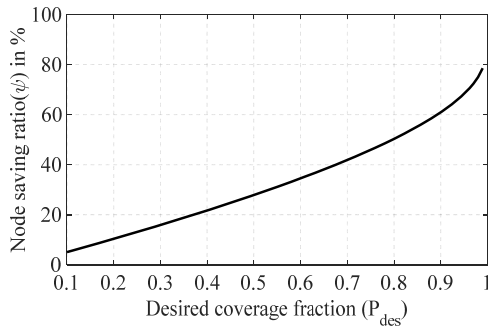


Fig. 10. Node saving ratio ( $\psi$ ) with the variation of desired coverage fraction ( $P_{des}$ ).

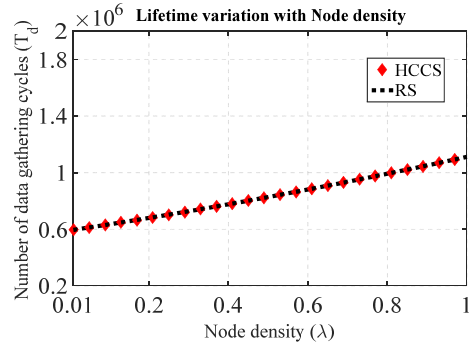


Fig. 11. Lifetime variation with node density for probabilistic HCCS and RS schemes.

Fig. 11 shows variation of number of data gathering cycle ( $T_d$ ) with varying node density ( $\lambda$ ) for different scheduling schemes. Here the system parameters used for network lifetime analysis are shown in Table 3. It is observed that the network lifetime increases with the increase in node density as expected. However, for higher node densities the increase in network lifetime is not much pronounced as the node density increases number of active nodes also increases, this on the other hand increases the overall energy consumption of the network. It is further observed that the lifetime curve for probabilistic HCCS scheme coincides with the curve for RS scheme. It can be concluded from the figure that though probabilistic HCCS scheme consumes additional energy due to transmission of communication overheads the network lifetime achieved by our proposed scheme is almost equal to the RS scheme.

**Table 3. System parameters considered for network lifetime analysis.**

Parameter	Value
Packet length, $B$	8 bits
Duration of data gathering cycle, $T_d$	500 secs
Path loss exponent, $\eta$	4.0
Power density of sensor node, $\alpha$	388 $\mu\text{W}/\text{m}^2$
$e_i$	0.05 $\mu\text{J}/\text{packet}$
$e_d(\eta=2)$	0.1 $\text{nJ}/\text{packet}/\text{m}^2$
Initial battery energy, $E_0$	23.760 kJ

## 7. CONCLUSIONS

In this paper, attempt has been made to develop a probabilistic hard-core coordinated scheduling scheme (HCCS) for sensor nodes using the concepts of hard-core point

process from stochastic geometry. In dense WSNs, signals emitted by the nodes for sensing task are affected by the interfering signals from nearby transmissions. In such environmental conditions, nodes are prone to become nonfunctional. The existing literature has addressed multiple sensor scheduling schemes, however have ignored the impact of inherent channel randomness on the achievable coverage during their study. The proposed probabilistic coordinated sensor scheduling based on inhibition distance reduces the energy consumption by activating minimum number of sensors using little communication overheads. We have further analyzed the influence of various sensing channel parameters and interferers on sensor activation probability.  $K$ -coverage is also ensured to the monitored region by adopting the sensing radius as the inhibition distance between two simultaneously active sensors. The combined effect of node failure and coverage degree on the coverage performance in presence of interference is also shown. The coverage fraction achieved by probabilistic HCCS scheme outperforms the RS scheme even in no node failure case by almost  $\sim 35\%$  at active sensor node density  $\lambda = 0.05/\text{m}^2$ , coverage degree  $K = 1$  and number of interferers  $k = 6$ . It can be concluded from the results that probabilistic HCCS scheme outperforms the RS scheme in the event of interference, node failure, and required coverage degree.

## REFERENCES

1. A. Hossain, S. Chakrabarti, and P. K. Biswas, "Impact of sensing model on wireless sensor network coverage," *IET Wireless Sensor Systems*, Vol. 2, 2012, pp. 272-281.
2. A. K. Singh, N. Purohit, and S. Varma, "Analysis of lifetime of wireless sensor network with base station moving on different paths," *International Journal of Electronics*, Vol. 101, 2015, pp. 605-620.
3. D. Tian and N. D. Georganas, "A coverage-preserving node scheduling scheme for large wireless sensor networks," in *Proceedings of the 1st ACM International Workshop on Wireless Sensor Networks Applications*, 2002, pp. 32-41.
4. H. M. Ammari and S. K. Das, "Centralized and clustered k-coverage protocols for wireless sensor networks," *IEEE Transactions on Computers*, Vol. 61, 2012, pp. 118-133.
5. J. Deng, Y. S. Han, W. B. Heinzelman, and P. K. Varshney, "Balanced-energy sleep scheduling scheme for high-density cluster-based sensor networks," *Computer Communications*, Vol. 28, 2005, pp. 1631-1642.
6. C. Qing, T. Abdelzaher, H. Tian, and J. Stankovic, "Towards optimal sleep scheduling in sensor networks for rare-event detection," in *Proceedings of the 4th International Symposium on Information Processing in Sensor Networks*, 2005, pp. 20-27.
7. B. Jiang, B. Ravindran, and H. Cho, "Energy efficient sleep scheduling in sensor networks for multiple target tracking," in *Proceedings of International Conference on Distributed Computing in Sensor Systems*, LNCS, Vol. 5067, 2008, pp. 498-509.
8. J. Deng, Y. S. Han, W. B. Heinzelman, and P. K. Varshney, "Scheduling sleeping nodes in high density cluster-based sensor networks," *Mobile Networks and Applications Special Issue on Energy Constraints and Lifetime Performance in Wireless Sensor Networks*, Vol. 10, 2005, pp. 825-835.

9. H. Jaleel and M. Egerstedt, "Sleep scheduling of wireless sensor networks using hard-core point processes," in *Proceedings of American Control Conference*, 2013, pp. 788-793.
10. A. Elfes, "Occupancy grids: A stochastic spatial representation for active robot perception," in S. S. Iyenger, A. Elfes, , eds., *Autonomous Mobile Robots: Perception, Mapping and Navigation*, Vol. 1, 1991, pp. 60-70.
11. Y. R. Tsai, "Sensing coverage for randomly distributed wireless sensor networks in shadowed environments," *IEEE Transactions on Vehicular Technology*, Vol. 57, 2008, pp. 556-564.
12. S. Kumar and D. K. Lobiyal, "Sensing coverage prediction for wireless sensor networks in shadowed and multipath environment," *Scientific World Journal*, Article ID 565419, 2013, 11 pages.
13. L. H. Yen, C. W. Yu, and Y. M. Cheng, "Expected  $k$ -coverage in wireless sensor networks," *Ad Hoc Networks*, Vol. 4, 2006, pp. 636-650.
14. Z. Zhou, S. Das, and H. Gupta, "Connected  $k$ -coverage problem in sensor networks," in *Proceedings of the 13th International Conference on Computer Communications and Networks*, 2004, pp. 373-378.
15. A. K. Sagar and D. K. Lobiyal, "Fault tolerant coverage and connectivity in presence of channel randomness," *Scientific World Journal*, Vol. 2014, 2014.
16. R. R. Patra and P. K. Patra, "Analysis of  $k$ -coverage in wireless sensor networks," *International Journal of Advanced Computer Science and Applications*, Vol. 2, 2011, pp. 91-96.
17. W. Ye, J. Heidemann, and D. Estrin, "An energy efficient MAC protocol for wireless sensor networks," in *Proceedings of the 21st Annual Joint Conference of IEEE Computer and Communications Societies*, 2002, pp. 1567-1576.
18. C. Hsin and M. Liu, "Network coverage using low duty-cycled sensors," in *Proceedings of the 3rd International Symposium on Information Processing in Sensor Networks*, 2004, pp. 433-442.
19. B. Singh and D. K. Lobiyal, "Traffic-aware density-based sleep scheduling and energy modeling for two dimensional gaussian distributed wireless sensor network," *Wireless Personal Communication*, Vol. 70, 2013, pp. 1373-1396.
20. A. Adulyasas, Z. Sun, and N. Wang, "Connected coverage optimization for sensor scheduling in wireless sensor networks," *IEEE Sensors Journal*, Vol. 15, 2015, pp. 3877-3892.
21. H. P. Gupta, S. V. Rao, and T. Venkatesh, "Sleep scheduling protocol for  $\kappa$ -coverage of three-dimensional heterogeneous WSNs," *IEEE Transactions on Vehicular Technology*, Vol. 65, 2016, pp. 8423-8431.
22. Z. Chen, A. Liu, Z. Li, Y. J. Choi, and J. Li, "Distributed duty cycle control for delay improvement in wireless sensor networks," *Peer-to-Peer Networking and Applications*, Vol. 10, 2017, pp. 559-578.
23. P. Chen and W. Hu, "Sleep – wake up scheduling with probabilistic coverage model in sensor networks," *International Journal of Parallel, Emergent and Distributed Systems*, Vol. 29, 2014, pp. 1-16.
24. Q. Yang, S. He, J. Li, J. Chen, and Y. Sun, "Energy-efficient probabilistic area coverage in wireless sensor networks," *IEEE Transactions on Vehicular Technology*, Vol. 64, 2015, pp. 367-377.

25. K. Lin, L. Xiuhua, Z. Yinghai, W. Weidong, and L. Jinlan, "A  $k$ -coverage scheduling scheme in wireless sensor network based on hard-core process in Rayleigh fading channel," *China Communications*, Voll. 12, 2015, pp. 92-103.
26. M. Z. Win, P. C. Pinto, and L. A. Shepp, "A mathematical theory of network interference and its applications," *Proceedings of the IEEE*, Vol. 97, 2009, pp. 205-230.
27. S. Kumar and D. K. Lobiyal, "Impact of interference on coverage in wireless sensor networks," *Wireless Personal Communication*, Vol. 74, 2014, pp. 683-701.
28. D. C. Cox, "Cochannel interference considerations in frequency reuse small-coverage-area radio systems," *IEEE Transactions on Communications*, Vol. 30, 1982, pp. 135-142.
29. A. A. Dayya and N. C. Beaulieu, "Outage probabilities in the presence of correlated lognormal interferers," *IEEE Transactions on Vehicular Technology*, Vol. 43, 1994, pp. 164-173.
30. S. Debnath, A. Hossain, and S. M. Chowdhury, "Comment on impact of interference on coverage in wireless sensor networks," *Wireless Personal Communication*, Vol. 97, 2017, pp. 1071-1073.
31. J. Teichmann, F. Ballani, and K. G. van den Boogaart, "Generalizations of Matérn's hard-core point processes," *Spatial Statistics*, Vol. 3, 2013, pp. 33-53.
32. D. Stoyan, W. Kendall, and J. Mecke, *Stochastic Geometry and its Applications*, 2nd ed., Wiley, NY, 1996.
33. W. Li and W. Zhang, "Coverage analysis and active scheme of wireless sensor networks," *IET Wireless Sensor Systems*, Vol. 2, 2012, pp. 86-91.
34. A. K. Singh, S. Debnath, and A. Hossain, "Efficient deployment strategies of sensor nodes in wireless sensor networks," in *Proceedings of International Conference on Computational Techniques in Information and Communication Technologies*, 2016, pp. 694-698.
35. A. Hossain, T. Radhika, S. Chakrabarti, and P. K. Biswas, "An approach to increase the lifetime of a linear array of wireless sensor nodes," *International Journal of Wireless Information Networks*, Vol. 15, 2008, pp. 72-81.
36. A. Hossain, "Equal energy dissipation in wireless sensor network," *International Journal of Electronics and Communications*, Vol. 71, 2008, pp. 192-196.
37. M. Liu, J. Cao, W. Lou, L. Chen, and X. Li, "Coverage analysis for wireless sensor networks," in *Proceedings of International Conference on Mobile Ad-Hoc and Sensor Networks*, Vol. 3794, 2005, pp. 711-720.



**Sunandita Debnath** earned the Ph.D. degree in Electronics and Communication Engineering, from National Institute of Technology (NIT), Silchar, India in 2019. She is currently working as an Assistant Professor in the Department of Electronics and Communication Engineering, Madanapalle Institute of Technology and Science (MITS), Andhra Pradesh, India. Her research interests include wireless sensor network, mobile wireless sensor network.



**Ashraf Hossain** earned the Ph.D. degree in Electronics and Electrical Communication Engineering, from Indian Institute of Technology (IIT), Kharagpur, India in 2011. He is currently working as an Associate Professor in the Department of Electronics and Communication Engineering, National Institute of Technology (NIT), Silchar, India. His research interests include wireless sensor network, communication theory and systems. He is a senior member of IEEE and IE (India).